MECHANICAL PROPERTIES OF GRANULITE FROM HORNÍ BORY IN BOHEMIAN MASSIF

Dagmar HAVLÍČKOVÁ[1], Martin ZÁVACKÝ[1], Lukáš KRMÍČEK[1,2], Manfred BLÜMEL[3], Iva ROZSYPALOVÁ[4]
[1)]Brno University of Technology, Faculty of Civil Engineering, Institute of Geotechnics, Veveří 95, Brno, Czech Republic
[2)]Institute of Geology of the Czech Academy of Sciences, Rozvojová 269, CZ-165 02 Prague 6, Czech Republic
[3)]Institute for Rock Mechanics and Tunnelling, Graz University of Technology, Graz, Austria
[4)]Brno University of Technology, Faculty of Civil Engineering, Institute of Building Testing, Veveří 95, Brno, Czech Republic
E-mail: havlic.dag@gmail.com

ABSTRACT

Granulite represents one of the favourite rock types for the construction of an underground nuclear waste repository in the Czech Republic. Granulite from the Bohemian Massif (locality Horní Bory) was investigated in this study, with a special focus on the evaluation of the rock anisotropy. Investigated rock represents typical fine-grained foliated felsic granulite with principal mineral association: quartz + feldspar (K-feldspar > plagioclase) + garnet + biotite + kyanite and/or sillimanite. Anisotropy was identified in the rock fabric both at macroscopic and microscopic scale. During the laboratory testing, granulite reached considerable high uniaxial compressive strength (UCS) - up to 240 MPa; and brittle type (Class II) of failure occurred. We found that variability of the UCS and Young's modulus were relatively low. On the other hand, variability of the Poisson's ratio and the constants in Hoek-Brown failure criterion in triaxial loading were significantly high.

Keywords: granulite, mineral properties, foliation, uniaxial compressive strength, triaxial compressive strength, anisotropic properties

1 INTRODUCTION

Granulite is light crystalline, highly compact rock with biotite-bearing bands and disseminated garnet. It was originally recognized from the area of Bohemian Massif by von Justi in 1754 [1] under the name "Namiester Stein" on its type locality – Lamberk near Náměšť nad Oslavou (Náměšť Granulite Massif) and 48 years later characterised under the name "Weisstein" (white stone) from the Saxonian Granulite Massif (Sächsisches Granulitgebirge) as a light coloured rock with quartz + feldspar-dominated mineral assemblage [2] (Figure 1; Figure 2A, 2B). Granulites from the Bohemian Massif were more recently characterised in several papers [3, 4, 5, 6, 7]. This high-pressure and rarely microdiamond-bearing rocks [8], which holds a potential to record conditions of their formation deep in the Earth's crust, were selected as one of the promising rocks type for the construction of the deep-seated nuclear waste repository in the Czech Republic [9, 10 and references therein].

Foliated structure of granulite as high-pressure metamorphic rock can appear. This macroscopic structure of the rock indicates potential of anisotropy of mechanical properties. Influence of mechanical properties anisotropy regarding the design of nuclear waste repository was investigated in detail on gneiss in Finland [11]. Full description of anisotropy has 36 elastic constants of which 21 are independent in terms of the theory of elasticity by using the generalized form of Hooke's law. However, some simplification can be used in many practical cases. Transverse isotropy (five constants) is usually considered when a rock has isotropic properties in a plane normal to an axis of rotational symmetry. Orthotropy (nine constants) is usually considered, when three orthogonal planes of elastic symmetry exist at each point in a rock and these planes have the same orientation throughout the rock [12]. A comprehensive study of rock anisotropy based on 200 sets of tests results was carried out by Worotnicki [13]. Four groups of anisotropic rocks were established in the study: quartzofeldspathic rocks, basic/lithic rocks, pelitic rocks and carbonate rocks. About 70% of quartzofeldspathic rocks showed a relatively low degree of anisotropy with maximal to minimal Young's modulus ratio less than 1.3. Thus, we can assume that granulite as member of this rock group can show a relatively low degree of anisotropy.

Generally, there is a lack of relevant data about mechanical properties, i.e. combined uniaxial compressive strength, triaxial compressive strength, splitting tensile strength and testing of granulite rock that are accompanied by a detailed petrographic study. The principal aim of our study is to provide combined petrographic and mechanical characteristics of granulite samples from the Horní Bory quarry located within the Bory Granulite

Massif, the Czech Republic. The quarry is located near a potential site for the construction of an underground nuclear waste repository for spent nuclear fuel and radioactive waste.

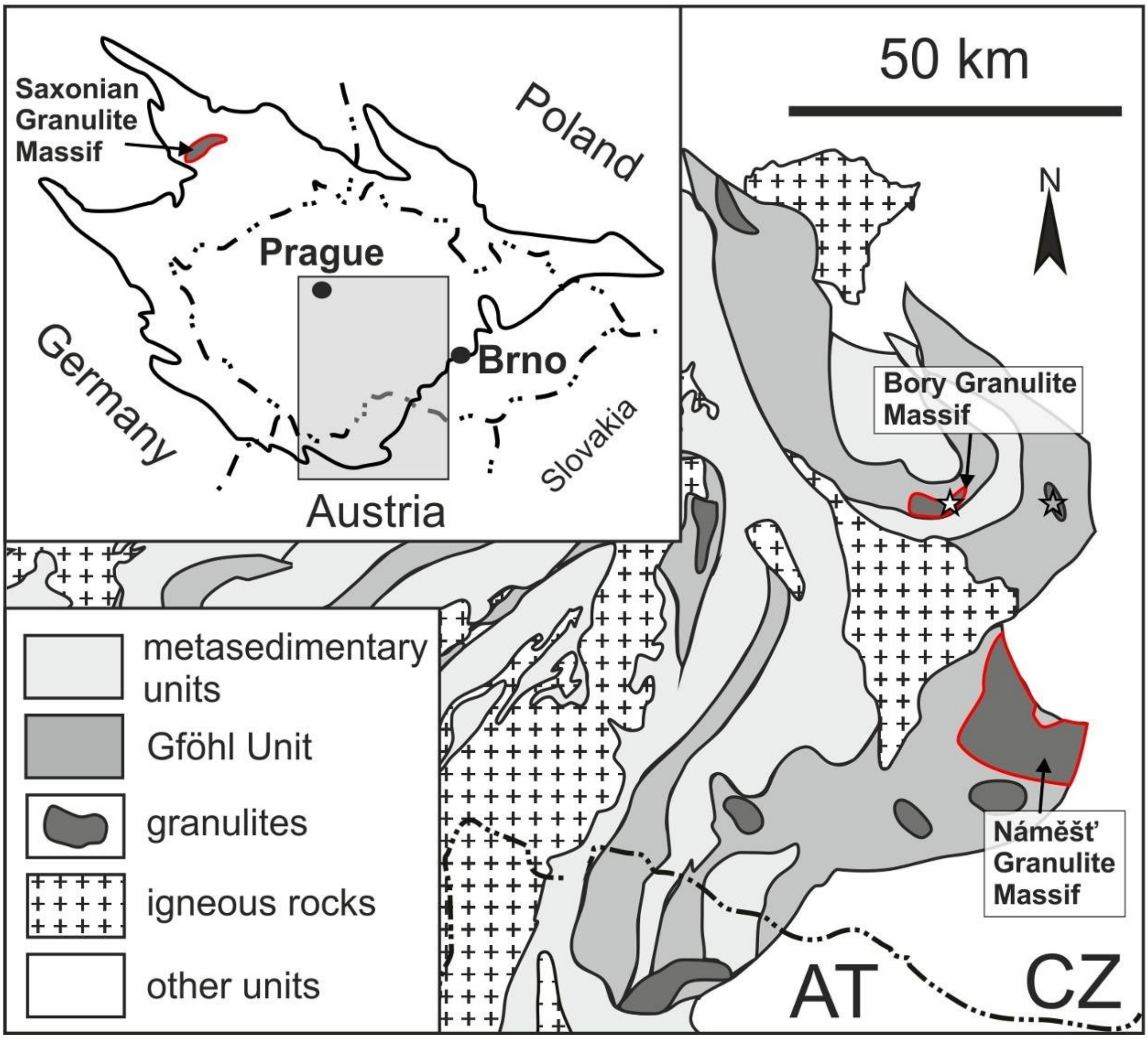

Figure 1. Schematic sketch of the Bohemian Massif with highlighted type granulite massifs (Náměšť Granulite Massif in the Czech Republic and Saxonian Granulite Massif in Germany) along with investigated Bory Granulite Massif on the south-eastern border of the Bohemian Massif [14, modified]. Position of the Horní Bory quarry is marked by white asterisk, and the location of the potential site (Kraví Hora) for the construction of underground nuclear waste repository is marked by grey asterisk

2 GEOLOGY OF STUDIED LOCALITY

The state owned company SURAO of the Czech Republic intends to build a deep geological repository for radioactive waste storage. It is a consensus that the waste repository will be located in crystalline rocks, similar to pilot projects in Sweden and Finland [15, 16]. The waste is planned to be stored up to a maximum depth of 500 m below surface [10]. Recently, several geologically suitable deposition sites have been identified [9], with two highly favourable sites: Horka near Velké Meziříčí in syenitic rocks [17 and references therein] and Kraví hora near Dolní Rožínka in granulitic rocks. Kraví hora (611 m a.s.l.), located near the village Střítež, is situated within 340 Ma granulite rocks of the lower-crustal Gföhl tectonostratigraphic Unit of the Strážek Moldanubicum [18] (Figure 1). The depth of the rock complexes is estimated to be several km [9 and references therein], which satisfies the requirements of repository depth. However, surface outcrops of ganulites are very scarce in the surroundings of the Kraví hora site, and the available is not sufficiently fresh for the complex assessment of its mechanical properties (Figure 2C). Thus, fresh granulite was investigated and sampled from nearby (ca 16 km W from Kraví hora site and 8 km from Velké Meziříčí) active Horní Bory quarry situated within Bory Granulite Massif (10 × 3.5 km in area) of the Strážek Moldanubicum [19] (Figure 1). In the quarry were sampled blocks of fine-grained variably foliated felsic granulites with mineral association: quartz + alkali-feldspar + plagioclase + garnet + biotite + kyanite and/or sillimanite (Figure 2D).

Volume LXV (2019), No. 4
p. 38 – 53, ISSN 1802-5420
DOI 10.35180/gse-2019-0022

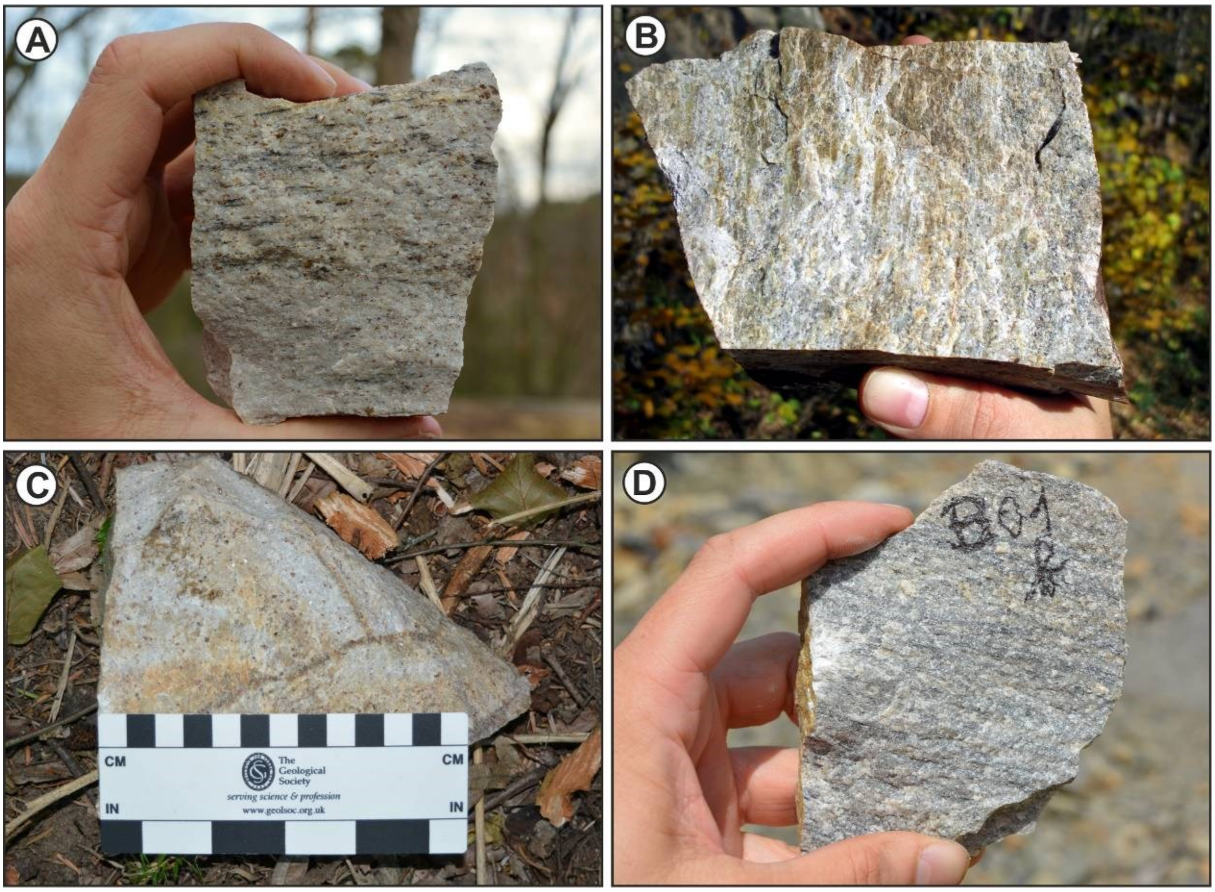

Figure 2. Examples of felsic granulites from the Bohemian Massif. A – Granulite sample from von Justi's type locality – Lamberk in the Náměšť Granulite Massif; B – Characteristic granulite from the Saxonian Granulite Massif (locality Sachsenburg); C – Weathered granulite from Kraví hora area, one of the potential sites for the construction of underground nuclear waste repository; D – Granulite fragment from investigated larger blocks sampled in Horní Bory active quarry

3 METHODS

3.1 Petrographic analysis

Tested granulite samples from Horní Bory were described petrographically using conventional optical microscopy. Furthermore, backscatter electron imaging (BSE) and compositional characteristic of main minerals (feldspar, garnet, and mica) were carried out using a CAMECA SX 100 electron microprobe at the Laboratory of Electron Microscopy and Microanalysis, jointly operated by the Masaryk University (Brno) and the Czech Geological Survey. Operating conditions for quantitative WDS analyses involved an accelerating voltage of 15 kV, beam currents 10 nA and a spot size ~5 µm. Both natural and synthetic minerals were used as reference standards. The X-phi correction procedure [20] was used for spectra processing. Mineral compositions and formulae are listed in atoms per formula units (apfu) and X_{Mg} [Mg/(Mg + Fe)]. Abbreviations of mineral names are used according to Whitney and Evans [21].

3.2 Mechanical parameters

Specimens for mechanical tests were collected and prepared from three blocks of the granulite rock (BO-A, BO-B and BO-C) sampled in quarry Horní Bory. This study is focused on preliminary evaluation of anisotropy of the granulite mechanical properties. However, as it was mentioned in introduction, full description of rock anisotropy is relatively complicated and requires comprehensive testing. Thus, the aim of our study is to describe and compare properties of the rock in two main directions: perpendicular and parallel with foliation planes. Main part of the tests was carried out in Laboratory of rock mechanics at Graz University of Technology. Additional fracturing tests were carried out in laboratory at Institute of Building Testing at Brno University of Technology. Cylindrical specimens were drilled with diameter of 50 mm and L:D ratio of 2.0 for uniaxial compressive strength (UCS) tests and triaxial compression tests. Notation of the specimens and their orientation during testing is summarized and explained in Table 1.

Volume LXV (2019), No. 4
p. 38 – 53, ISSN 1802-5420
DOI 10.35180/gse-2019-0022

Table 1. Specimen preparation for rock mechanics testing of granulites

Specimen	Test type	Note
BO-1a	UCS	Drilled perpendicular to foliation. Both from rock block BO-A.
BO-2a	Triaxial	
BO-1b	UCS	Drilled parallel with foliation. Both from rock block BO-C.
BO-2b	Triaxial	
BO02a1	Fracturing tests	Prepared from rock block BO-B.
BO02a2		Prepared from rock block BO-B.
BO03		Prepared from rock block BO-C.

Ultrasonic velocity was determined on the specimens before destructive tests. Set of measurement profiles was applied on each specimen (see Figure 3) in order to study the influence of foliation on the ultrasonic velocity. Travel time of P-wave ultrasonic impulses was recorded, and velocities were determined. Dynamic elastic modulus E_{dyn} was calculated according to formula (1) derived from equation of P-wave velocity in block specimen as stated in ISRM Suggested Method [22].

$$E_{dyn} = \rho {v_p}^2 \frac{1 - \nu - 2\nu^2}{1 - \nu} \qquad \textbf{(1)}$$

where ρ is density, v_p is ultrasonic velocity and ν is Poisson's ratio.

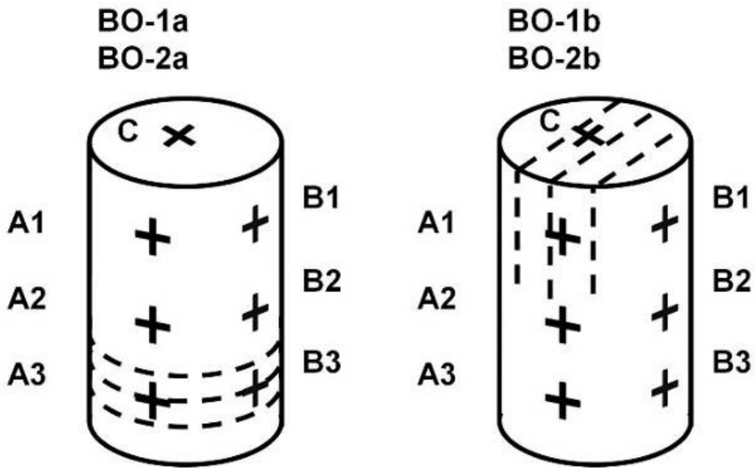

Figure 3. Ultrasonic velocity measuring profiles. The dashed line shows foliation orientation

The samples used for the UCS tests were equipped with two axial strain and one circumferential LVDT strain gauge sensors. Radial strain was calculated from log of the circumferential deformation. One unloading and reloading loop was applied in the beginning of each UCS test. The specimen was loaded to 34 MPa, then unloaded to 10 MPa and reloaded to 34 MPa. The test was stress controlled in this phase with a load rate of 0.4 MPa/s. Thereafter the test was deformation controlled by the circumferential deformation rate of 0.05 mm/min. This control mode allows to obtain the post-peak behaviour for class II rock types.

The unloading and reloading procedure was used in order to determine deformability parameters of the rock. The deformation modulus E_{def} was determined as secant modulus between two points of stress-strain diagram. The points were considered where 10 MPa and 34 MPa of the axial stress was reached for the first time. Young's modulus E and the Poisson's ratio ν were determined as average from secant value of the unloading and reloading parts of the loop.

Triaxial compression tests were carried out on two specimens with respect to the foliation orientation. Multiple failure state procedure was employed in order to obtain necessary amount of data for failure envelope analysis. The multiple failure procedure is described in ISRM suggested method [23] and it is well established in Laboratory of rock mechanics at Graz University of Technology [24].

Volume LXV (2019), No. 4
p. 38 – 53, ISSN 1802-5420
DOI 10.35180/gse-2019-0022

Parameters of Hoek-Brown failure criterion (see formula 2) were determined in order to evaluate the influence of the foliation orientation within triaxial load conditions [25]. The parameter values were found by spreadsheet calculation.

$$\sigma_1 = \sigma_3 + \sigma_{ci}\left(m_i \frac{\sigma_3}{\sigma_{ci}} + s\right)^a \quad (2)$$

where σ_1 and σ_3 are major and minor principal stresses, σ_{ci} is uniaxial compressive strength and m_i, s, a are material constants. The σ_{ci} and m_i were determined by method of least squares while conventional values of the s and a were considered for the case of intact rock.

The tensile strength was determined by splitting tensile test. The test was carried out on three disc specimens. The foliation planes were oriented perpendicular to the surface of the load platen and perpendicular to the drilling core longitudinal axis. Average value of the tensile strength was determined.

Fracturing tests were carried out in a set-up of 3-point bending tests according to ISRM Suggested Method [26]. Hence, the tensile mode of fracture, commonly referred to as mode I fracture toughness testing, was investigated. Round bar specimens were used with diameter 50 mm and length 200 mm. A chevron notch was created in the mid-span as the stress concentrator. The test was conducted as deformation controlled with rate 0.01 mm/min. Foliation planes were oriented parallel with the specimen longitudinal axis and transversal inclination of the planes was approximately 45°. Fracture toughness K_{IC} was calculated by the formula (3) [26].

$$K_{CI} = \frac{A_{\min} F_{max}}{D^{1.5}} \quad (3)$$

where F_{max} is the maximal reached load, D is diameter of the specimen and A_{min} is calculated according formula (4):

$$A_{min} = \frac{\left[1.835 + \frac{7.15a_0}{D} + 9.85\left(\frac{a_0}{D}\right)^2\right]S}{D} \quad (4)$$

where a_0 is chevron tip distance from specimen surface and S is distance between supports.

4 RESULTS

4.1 Petrographic characteristics

Principal mineral association of the studied granulites consist of quartz, feldspar (K-feldspar > plagioclase), garnet, biotite, kyanite/sillimanite, with accessory ilmenite, apatite, hercynite and zircon. The granulites from Horní Bory quarry are characterized by porphyroblasts of garnet with predominance of the almandine component (Figure 4 and 5; Table 2). Variably foliated samples contain biotite (X_{Mg}~0.4) along foliation planes (Figure 4 and 5A; Table 3). Quartz forms irregular, elongated aggregates and occasionally forms myrmekitic intergrowth with feldspar as well. K-feldspar is anhedral and significantly perthitic. Its compositional range is shown in Figure 6B and listed in Table 3. Plagioclase, by its composition, mainly corresponds to oligoclase. Garnet porphyroblasts are present as rounded, colourless grains, which are sometimes heavily cracked. Kyanite often changes to acicular sillimanite (Figure 4C and Figure 5D). Rutile creates typical yellow-brown micro-porphyroblasts with striking relief. Ilmenite shows signs of leucoxenization at the edges and breaks down into finer material (Figure 5A). Apatite is present in the form of elongated grains.

Volume LXV (2019), No. 4
p. 38 – 53, ISSN 1802-5420
DOI 10.35180/gse-2019-0022

Table 2. Representative composition of garnet in granulite from Horní Bory

No.	1	2	3	4
Rock type	granulite	granulite	granulite	granulite
P_2O_5	0.28	0.13	0.18	0.15
SiO_2	37.0	37.1	37.1	37.1
Al_2O_3	21.1	20.9	20.9	21.1
MgO	3.37	3.34	3.52	3.35
CaO	0.70	0.53	0.57	0.45
MnO	2.16	2.18	2.20	2.27
FeO	36.0	36.0	36.1	36.2
Total	100.7	100.1	100.5	100.5
Empirical formula (apfu) on the basis of 8cat. and 12O				
P	0.02	0.01	0.01	0.01
Si	2.97	2.99	2.98	2.98
Al^{IV}	0.03	0.01	0.02	0.02
Al	1.99	1.98	1.97	1.99
Al^{VI}	1.96	1.97	1.95	1.97
Fe^{III}	0.02	0.01	0.04	0.02
Mg	0.40	0.40	0.42	0.40
Ca	0.06	0.05	0.05	0.04
Mn	0.15	0.15	0.15	0.15
Fe^{II}	2.40	2.41	2.38	2.40
Fe^{tot}	2.42	2.42	2.42	2.43

Y, K, Ti and Cr are below their detection limits.

Table 3. Representative composition of dark mica in granulite from Horní Bory

No.	1	2	3
Rock type	granulite	granulite	granulite
SiO_2	36.1	35.8	35.6
TiO_2	2.86	3.18	3.47
Al_2O_3	18.9	19.0	18.9
MgO	7.86	7.76	7.46
MnO	0.08	0.10	0.07
FeO	20.7	20.8	20.9
BaO	0.00	0.08	0.07
H_2O	3.46	3.49	3.49
Na_2O	0.14	0.13	0.09
K_2O	9.53	9.52	9.50
F	1.03	0.98	0.93
Cl	0.03	0.04	0.04
O = -F	-0.43	-0.41	-0.39
O = -Cl	-0.01	-0.01	-0.01

Volume LXV (2019), No. 4
p. 38 – 53, ISSN 1802-5420
DOI 10.35180/gse-2019-0022

Total	100.2	100.5	100.0
Empirical formula (apfu) on the basis of 11O			
Si	2.73	2.71	2.71
Ti	0.16	0.18	0.20
Al^{IV}	1.27	1.29	1.29
Al	1.69	1.70	1.69
Al^{VI}	0.42	0.41	0.40
Mg	0.89	0.88	0.85
Mn	0.01	0.01	0.00
Fe	1.31	1.32	1.33
Na	0.02	0.02	0.01
K	0.92	0.92	0.92
OH	1.75	1.76	1.77
F	0.25	0.23	0.22
O	10.1	10.1	10.1
Mg/(Mg + Fe)	0.40	0.40	0.39

Cr, V and Zn are below their detection limits.

Table 4. Representative composition of feldspar in granulite from Horní Bory

No.	1	2	3	4	5
Rock type	granulite	granulite	granulite	granulite	granulite
P_2O_5	0.22	0.33	0.38	0.73	0.42
SiO_2	65.8	63.7	65.1	63.4	65.2
Al_2O_3	21.2	18.9	21.8	19.1	21.8
CaO	1.92	0.04	2.40	0.02	2.28
FeO	0.00	0.00	0.14	0.00	0.05
PbO	0.03	0.00	0.07	0.00	0.00
Na_2O	10.4	1.37	10.1	1.56	10.4
K_2O	0.20	15.1	0.17	14.9	0.39
Total	99.7	99.5	100.1	99.8	100.4
Empirical formula (apfu) on the basis of 8O					
P	0.01	0.01	0.01	0.03	0.02
Si	2.99	2.90	2.96	2.88	2.96
Al	1.13	1.01	1.17	1.02	1.17
Ca	0.09	0.00	0.12	0.00	0.11
Fe	0.00	0.00	0.01	0.00	0.00
Na	0.92	0.12	0.89	0.14	0.91
K	0.01	0.88	0.01	0.87	0.02
Mol. %					
Or	1	88	1	86	2
Ab	90	12	88	14	87
An	9	0	11	0	11

Volume LXV (2019), No. 4
p. 38 – 53, ISSN 1802-5420
DOI 10.35180/gse-2019-0022

Rb, Sr, Pb, Ba are below their detection limits.

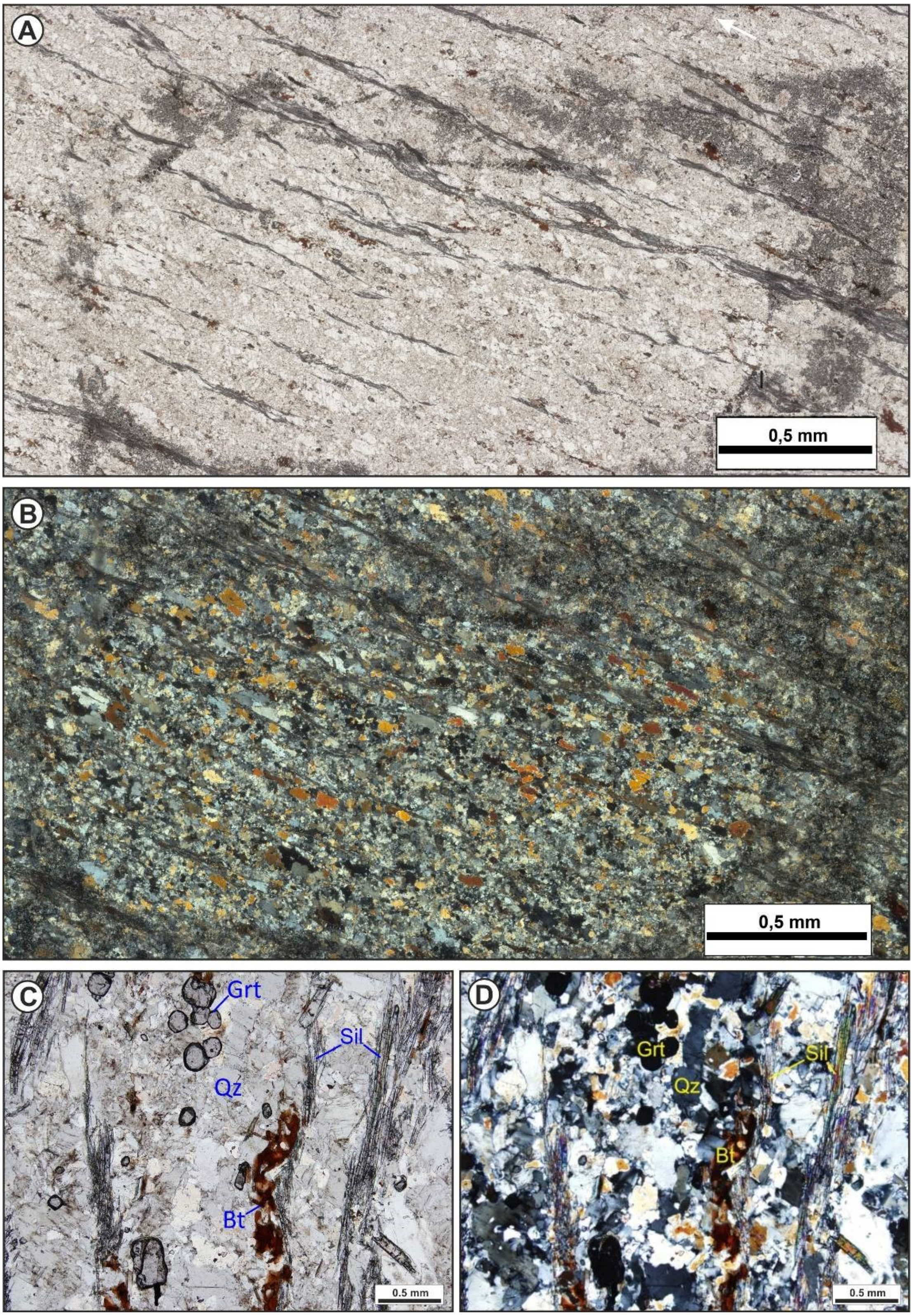

Figure 4. Principal petrographic features of granulites from Horní Bory. A – Overall mineral distribution in studied granulite with predominant mineral orientation (PPL); B – Same microphotograph as (A) with visible granoblastic texture (XPL); C – Detailed view on mineral composition with Bt (biotite), Grt (garnet), Sil (sillimanite) and Qz (quartz), PPL. D – Same microphotograph as (C) (XPL). PPL = plane-polarised light; XPL = crossed polarised light

Volume LXV (2019), No. 4
p. 38 – 53, ISSN 1802-5420
DOI 10.35180/gse-2019-0022

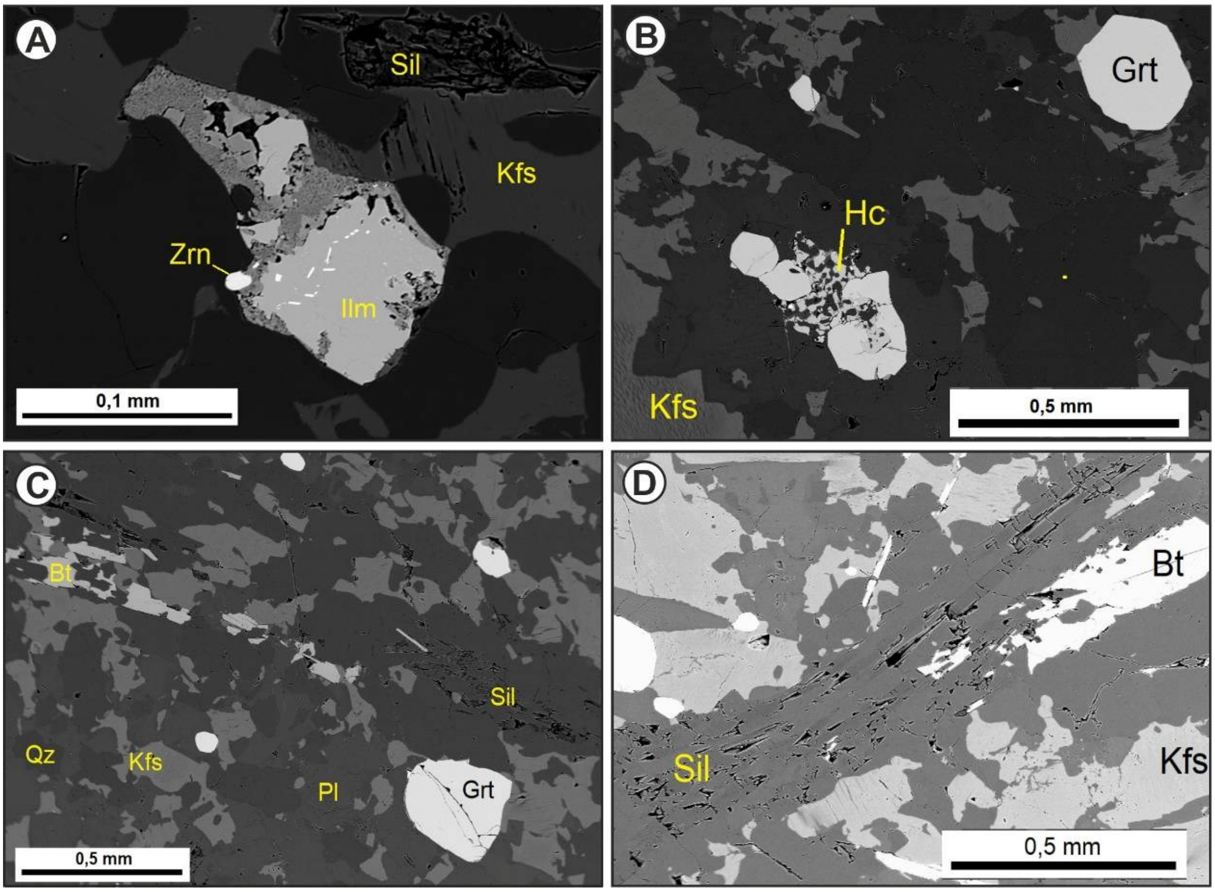

Figure 5. Principal BSE characteristics of granulite from Horní Bory. A – Ilmenite (Ilm) alterated into fine-grained material; B – Hercynite (Hc) together with broken garnet (Grt). C – Oriented biotite laths (Bt), garnet (Grt) and sillimanite (Sil) sitting in the matrix composed of K-feldspar (Kfs), plagioclase (Pl) and quartz (Qz); D – Grains of acicular sillimanite (Sil) along with biotite (Bt) and K-feldspar (Kfs)

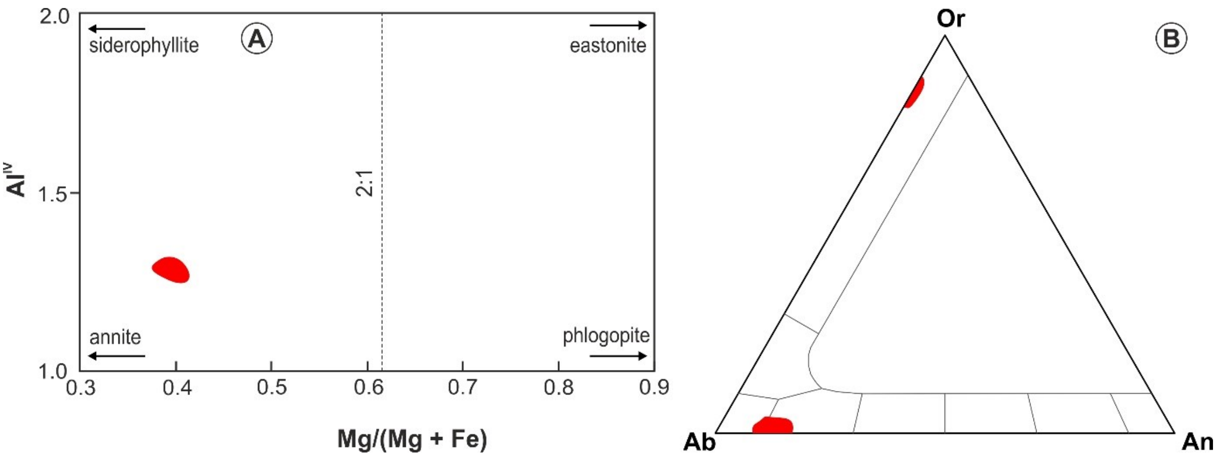

Figure 6. A – Position of feldspars from granulite samples from Horní Bory. B – positions of the dark mica from the Horní Bory granulite samples in the classification diagram for micas [27]

4.2 Mechanical properties and parameters

<u>*UCS testing*</u>. An overview of the main mechanical parameters is given in Table 5. Variation of the obtained values can be noticed according to the orientation of foliation. Granulite provided higher UCS when it was loaded perpendicular to foliation than parallel. Vice versa, the rock appeared slightly stiffer in case of loading parallel with foliation. This can be recognized according to the determined deformability parameters.

Volume LXV (2019), No. 4
p. 38 – 53, ISSN 1802-5420
DOI 10.35180/gse-2019-0022

Table 5. Physical and mechanical properties of the tested granulite

Orientation to foliation:	perpendicular	parallel	Units:
Density	2640		kg/m^3
UCS	240	225	MPa
E_{def}	62.6	64.8	GPa
Young's modulus, E	70.3	71.6	GPa
Poisson's ratio,ν	0.19	0.14	-
Tensile strength*	15.1		MPa

*orientation of foliation perpendicular to the loading platen and perpendicular to the drilling core longitudinal axis

Investigated granulite has relatively high strength (> 200 MPa) in UCS testing. Brittle failure of the rock was observed in both cases of foliation orientation accompanied by plummet of the peak-stress of the stress-strain curve (Figure 7). The control mode for this test procedure was a constant circumference ramp increase. This enables to control such a test for class II rocks in the post peak area. The plummet magnitude was more noteworthy at BO-1a specimen (Figure 7A). However, the plummet of the stress-strain curve at BO-1b specimen appeared immediately after reaching the peak strength (Figure 7B), when large crack formed along one of the foliation planes.

Variability of failure process was recognized by detailed strain analysis as well (Figure 8). Non-linear trend of radial and volumetric strain components appeared prior to peak UCS approaching during the complete test procedure of the two specimens (Figure 8). The most significant contrast appeared on volumetric strain (Figure 8 – curve 2). It can be quantified by position of minimal absolute volume point in the graph. The point is located where trend of volumetric strain is reversed, and the volumetric strain starts to decrease. Minimal absolute volume of BO-1a specimen was reached at 206 MPa (86 % of UCS) and for BO-1b specimen was reached at 219 MPa (97 % of UCS) and close to the peak strength.

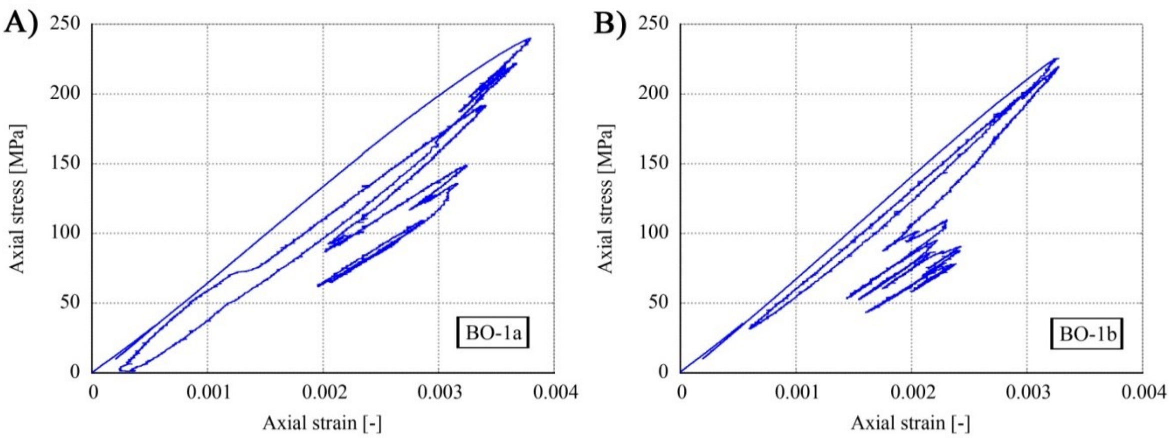

Figure 7. Complete stress-strain diagram of the UCS tests on granulite. Axial stress *versus* strain with peak strength and post-failure phase is plotted. A, sample BO-1a. B, sample BO-1b

Volume LXV (2019), No. 4
p. 38 – 53, ISSN 1802-5420
DOI 10.35180/gse-2019-0022

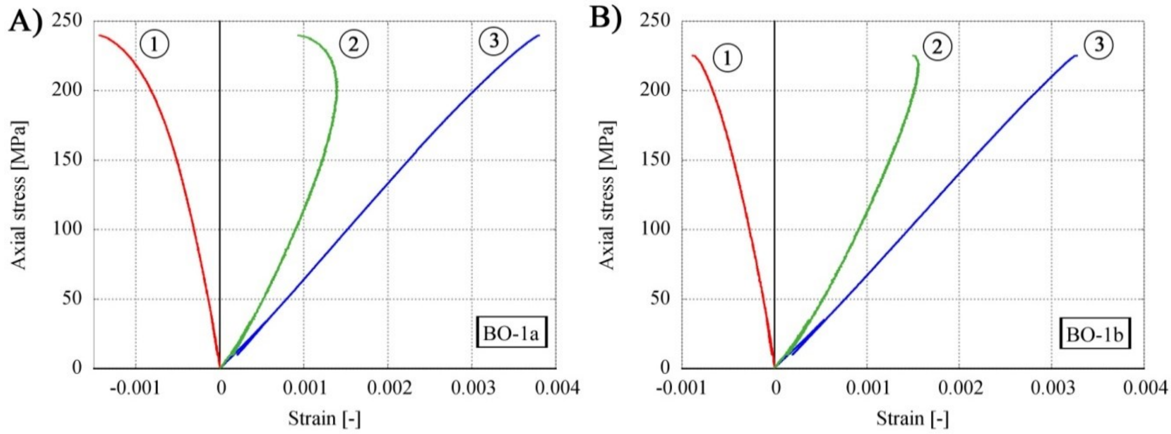

Figure 8. Stress-strain diagrams from the first loading cycle of the UCS tests with distinguished components of strain plotted to peak strength. Curve 1 – radial strain; curve 2 – volumetric strain; curve 3 – axial strain

Ultrasonic velocity test results. Determination of the dynamic elastic modulus (E_{dyn}) is based on ultrasonic velocity measurement (Table 6). Values of the E_{dyn} are summarized in Table 7. Values of density and Poisson's ratio for calculations were derived from Table 5. Foliation direction was considered for selection of value of Poisson's ratio. The general trend shows that E_{dyn} is higher in direction parallel with foliation (64.3 GPa in average) than in perpendicular direction (57.7 GPa in average). Deviation of dynamic modulus for specimen BO-2a is explained by the occurrence of a major crack close to one of the measurement profiles. Ultrasonic velocity was lowered by the crack formation, thus, E_{dyn} value became lower in this case.

Table 6. Ultrasonic test. (note: av. means average value)

Specimen	Ultrasonic velocity determined in profiles denoted according Figure 3 [km/s]								
	A1	A2	A3	B1	B2	B3	C	A av.	B av.
BO-1a	5.54	5.00	4.95	5.05	5.15	4.95	5.10	5.17	5.05
BO-1b	4.66	5.13	5.24	4.84	4.88	4.88	5.20	5.01	4.87
BO-2a	4.99	4.80	5.36	4.06	4.71	5.09	4.83	5.05	4.62
BO-2b	4.98	5.13	5.24	4.93	4.70	4.74	5.19	5.12	4.79

drilling core longitudinal axis: a - perpendicular to foliation; b - parallel with foliation

Table 7. Calculated dynamic elastic modulus E_{dyn} values [GPa] from velocity measurements. (note: * E_{dyn} determined in direction perpendicular to foliation; other parallel with foliation)

Specimen	A av.	B av.	C
BO-1a	67.2	64.3	62.5 *
BO-1b	63.2	56.9 *	68.1
BO-2a	64.2	53.8	56.1 *
BO-2b	65.9	55.2 *	67.9

Triaxial testing. Specimen BO-2a performed higher strength in multiple failure triaxial test, than BO-2b specimen (Figure 9). The peak strength shows the same feature regarding foliation orientation dependency as for the UCS test results. Contrast of radial strain curves should be noted in the stress-strain diagrams from the triaxial testing. Radial shrinkage was observed in specimen BO-2b when confining pressure was increased (Figure 9B). Values of peak axial stresses for different confining pressures reached during triaxial compression tests are listed in Table 8.

Volume LXV (2019), No. 4
p. 38 – 53, ISSN 1802-5420
DOI 10.35180/gse-2019-0022

Table 8. Peak stresses reached during triaxial testing of foliated granulite

Confining pressure	Peak axial stress σ_1 [MPa]	
σ_3 [MPa]	BO-2a	BO-2b
0*	240*	225*
5	298	236
10	353	259
13.5	391	272
20	470	301

* UCS tests on specimens BO-1a and BO-1b

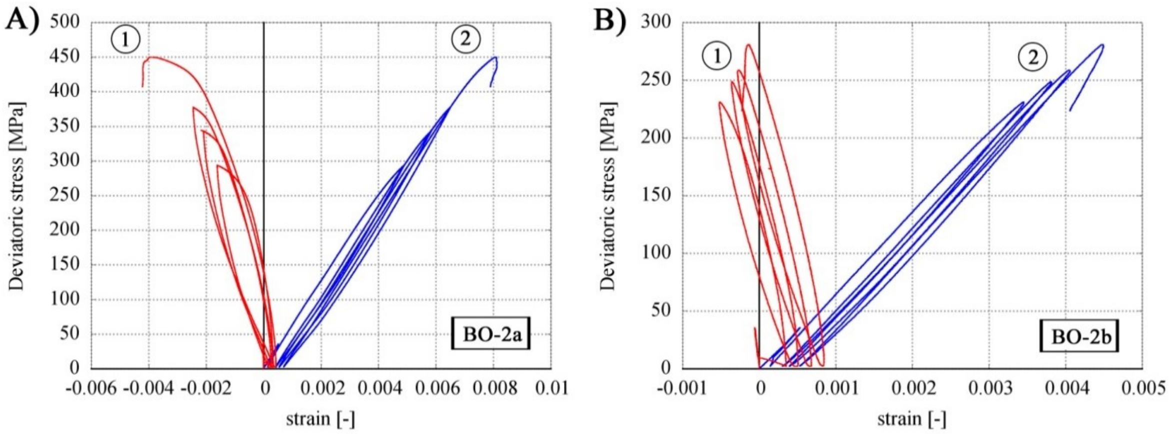

Figure 9. Stress-strain diagram of multiple failure state from triaxial testing. Curve "1" – radial strain; curve "2" – axial strain. A, specimen BO-2a loaded perpendicular to foliation. B, specimen BO-2b loaded parallel with foliation. Notice the much higher peak strength of specimen BO-2a

The data in Table 8 were further analysed in order to determine the parameters of the Hoek-Brown failure criterion and summarised in Table 9. Values of UCS were considered in the analysis as well. The parameter σ_{ci} is slightly underestimated by the Hoek-Brown criterion compared to directly determined UCS from testing. Variation of UCS is 3% for testing perpendicular to foliation and 2% at loading parallel with orientation of foliation. Material constant m_i in the criterion is significantly influenced by foliation orientation. The constant is considerably lower in direction parallel with the foliation. Tensile strength σ_t is estimated to be significantly lower in direction perpendicular to the foliation. Thus, influence of foliation orientation is also evident in case of tensile strength σ_t.

Table 9. Estimated parameters of Hoek-Brown failure criterion from triaxial and UCS testing and with consideration of foliation orientation

Parameter	Symbol	perpend.	parallel	Unit
Uniaxial compressive strength of intact rock	σ_{ci}	233	220	MPa
Material constants (standard values of s, a for intact rock are used)	m_i	29.5	6.4	-
	s	1.0	1.0	-
	a	0.5	0.5	-
Estimated tensile strength	σ_t	7.9	33.5	MPa

Fracture mechanics. The fracture toughness in tensile mode has relatively high value, in average 2.19 MPa.m$^{0.5}$. Results of the individual tests are listed in Table 10. Sample BO03 reached notably lower values than samples BO02a1 and BO02a2. This variance should be explained by natural variability of the rock properties, because the BO02-- samples were prepared from one and the same rock block.

Volume LXV (2019), No. 4
p. 38 – 53, ISSN 1802-5420
DOI 10.35180/gse-2019-0022

Table 10. Fracture toughness K_{IC} [MPa.m$^{0.5}$]

Specimen	BO02a1	BO02a2	BO03
Fracture toughness	2.29	2.33	1.97
Average	2.19		

5 DISCUSSION

5.1 Granulite petrographical features

Based on the observed mineral and petrographic composition we can state that the studied rock material corresponds to fine-grained, variably foliated, felsic granulite with principal mineral association: quartz + feldspar (K-feldspar > plagioclase) + garnet + biotite + kyanite and/or sillimanite and accessory ilmenite, apatite, hercynite and zircon. On the other hand, the rock does not texturally/mineralogically correspond to granulite gneiss, which can form layers, several centimetres to meters thick, in the Horní Bory granulite body [19 and discussion in sub-chapter 5.2.]. Thus, our tested material corresponds to granulite, which is the same petrographic type as is suggested for the construction of an underground nuclear waste repository [9].

5.2 Anisotropy of mechanical properties

Anisotropy of mechanical properties of the granulite from Horní Bory quarry was expected considering the foliation observed in microscopic and macroscopic scale. Some variation of the compressive strength and deformability parameters exist in the specimens studied. The UCS was of 6.3% higher in loading direction perpendicular to the foliation compared with the specimens loaded parallel with the foliation (see Table 5). Peak strengths reached from triaxial compression testing were much higher from loading perpendicular the foliation orientation (see Table 8). Parameter m_i of the Hoek-Brown failure criterion varied most significantly (78%). However, variation of the estimated tensile strength σ_t was also high (76%), but having an opposite trend – the strength was higher in tension from bending in the direction parallel with the foliation (see Table 9). When we compare deformability parameters, E (1.8%), E_{def} (3.4%) (see Table 5) and average of E_{dyn} (10%) (see Table 7) we observed slightly higher values when the foliation is oriented parallel with loading. The Poisson's ratio ν is 26% lower when the orientation of foliation is parallel with loading direction (see Table 5). Other findings of this study about tensile strength σ_t, modulus of elasticity and the Poisson's ratio with respect to influence of foliation orientation are in accordance with previous study of anisotropic metamorphic rocks presented by Brosch et al. [28]. To sum up, the degree of anisotropy of the specimen studied is relatively low, except for the m_i and σ_t parameters. The compressive strength under uniaxial and triaxial loading conditions decrease when the rock is loaded parallel with foliation, while E modules are slightly increased.

The tested granulite reached relatively high UCS (225 resp. 240 MPa – see Table 5). Hence, the rock belongs to grade "R5 - Very strong" of the ISRM classification [29] and the obtained UCS value is close to the upper limit of this grade (100–250 MPa). Brittle failure occurred especially during the UCS tests and agrees with the post-failure phase of the stress-strain diagrams presented in Figure 7. The obtained fracture toughness K_{IC} value is exceptionally high, as well. The reached value of 2.19 MPa.m$^{0.5}$ is significantly higher compared to the values reported for the 3-point bending experimental setup presented in the comprehensive list of results by Ouchterlony [26]. Fracture toughness of granulite is comparable with K_{IC} of igneous rocks like tonalite (2.21 MPa.m$^{0.5}$), dolerite (2.48 MPa.m$^{0.5}$) and basalt (2.01 MPa.m$^{0.5}$) [30].

Mechanical properties of granulite from the Bohemian Massif are reported in a recent study by Petružálek [31]. The study presents the UCS = 215 MPa, Young's modulus E = 49.8 MPa, and the Poisson's ratio ν = 0.19. The peak strength in triaxial compression testing is 310 MPa at confining pressure σ_3 = 13 MPa and the splitting tensile strength 10.5 MPa. The UCS, E and splitting tensile strength are lower than we obtained in our experiments. The Poisson's ratio reached the same value as in our study when the foliation was oriented perpendicular to loading direction. Peak strength in the triaxial tests is between values which we obtained (272 and 391 MPa – Table 8) at the most similar confinement (σ_3 = 13.5 MPa). Below we present a likely explanation of the difference in results of the two studies:

- Pertužálek [31] tested samples directly from Kraví Hora – potential location of the nuclear waste repository (see grey asterisk in Figure 1). The rock was sampled from available outcrops; thus, the rock could be weathered (cf. Figure 2C and 2D).
- Samples from Kraví hora site are strongly foliated [31 and figures therein] and more melanocratic than is characteristic for typical felsic granulite (cf. Figure 2). Higher content of dark minerals in the rock from Kraví hora site is indicated by its higher density (2655 kg/m^3) than we obtained in our study (Table 5). Hence, the rock from Kraví hora site resembles granulite gneiss, rather than granulite. This

Volume LXV (2019), No. 4
p. 38 – 53, ISSN 1802-5420
DOI 10.35180/gse-2019-0022

emphasizes the importance of detailed petrographic description along with reporting results of mechanical properties of rock.

6 CONCLUSIONS

Fine-grained variably foliated felsic granulite from the Bohemian Massif (locality Horní Bory) was investigated in this study, with a special focus on the evaluation of the rock anisotropy. Detailed study of petrography and mineralogy was done together with a set of mechanical tests. This rock represents one of the favourite rock types for the construction of underground nuclear waste repositories in the Czech Republic.

The main conclusions are summed up:

1. Anisotropy of granulite was identified in the rock fabric both at macroscopic and microscopic scale. Anisotropy of the mechanical properties appeared from testing the rock, as well. Variability of UCS and E modules was found to be relatively low. On the other hand, the variability of Poisson's ratio and the parameters of the Hoek-Brown failure criterion in triaxial load conditions is significantly high.
2. The tested granulite reached considerable high UCS (up to 240 MPa) and brittle type of failure (Class II) was observed during the laboratory testing. Brittleness of rock can lead to specific problems such as rock burst, thus, it should be considered as a potential risk during construction of underground openings of repositories.
3. Determination of mechanical properties of anisotropic rock requires considerably more laboratory data than could be presented in this study. Therefore, the presented quantification of the granulite anisotropy of the Horní Bory quarry should be considered as work in progress.

ACKNOWLEDGMENTS

This paper was written under the support of Brno University of Technology – Faculty of Civil Engineering, within grant No. FAST-S-19-6031, and the project No. LO1408 "AdMaS UP - Advanced Materials, Structures and Technologies", supported by the Ministry of Education, Youth and Sports under the "National Sustainability Programme I". The laboratory testing conducted at Graz University of Technology was part of project No. CZ.02.2.69/0.0/0.0/16_027/0008371. We thank Ove Stephansson (GFZ German Research Centre for Geosciences) for his very constructive and helpful comments and suggestions.

REFERENCES

[1] von JUSTI, J.H.G. Nachricht von einer neuen Art eines neues Halbedelgesteines so kürtzlich in Mähren entdeckt worden. *Neue Wahrheiten zum Vorteil der Naturkunde und des gesellschaftlichen Leben der Menchen 1*. 1754.

[2] ENGELBRECHT, Ch.A. Kurze Beschreibung des Weisssteins, einer im geognostischen System bis jetzt unbekannt gewesenen Gebirgsart. Schr. Linneschen Gesell. Leipzig. 1802.

[3] RÖTZLER, J. and R.L. ROMER. P–T–t evolution of ultrahigh temperature granulites from the Saxon Granulite Massif, Germany. Part I: Petrology. *Journal of Petrology*. 2001, 42, pp.1995-2013. DOI: 10.1093/petrology/42.11.2015.

[4] O'BRIEN, P.J. and J. RÖTZLER. High-pressure granulites: formation, recovery of peak conditions and implications for tectonics. *Journal of Metamorphic Geology*. 2003, 21, 1, pp.3-20. DOI: 10.1046/j.1525-1314.2003.00420.x.

[5] O'BRIEN, P.J. Type-locality granulites: high-pressure rocks formed at eclogite-facies conditions. *Mineralogy and Petrology*. 2006, 86, pp.161-175. DOI: 10.1007/s00710-005-0108-2.

[6] KOTKOVÁ, J. High-pressure granulites of the Bohemian Massif: recent advances and open questions. *Journal of Geosciences*. 2007, 52, pp.45-71. DOI: 10.3190/jgeosci.006.

[7] SAGAWE, A., A. GAERTNER, U. LINNEMANN, M. HOFMANN and A. GERDES. Exotic crustal components at the northern margin of the Bohemian Massif—Implications from U–Th–Pb and Hf isotopes of zircon from the Saxonian Granulite Massif. *Tectonophysics*. 2016, 681, pp.234-249. DOI: 10.1016/j.tecto.2016.04.013.

[8] KOTKOVÁ, J., P.J. O'BRIEN AND M. ZIEMANN. Diamond and coesite discovered in Saxony-type granulite: Solution to the Variscan garnet peridotite enigma. *Geology*. 2011, 39, pp.667–670. DOI: 10.1130/G31971.1.

[9] KOVÁČIK M., J. URÍK, M. ELIÁŠ, L. VONDROVIC, M. VENCL and I. POSPÍŠKOVÁ. *Ověření vhodnosti horninového prostředí pro umístění hlubinného úložiště VJP a RAO v PÚ ZZZK Březový potok, Čertovka, Čihadlo, Horka, Hrádek, Kraví hora a Magdaléna* (*Verification of rock environment suitability for an*

underground repository VJP and RAO in PÚ ZZZK Březový potok, Čertovka, Čihadlo, Horka, Hrádek, Kraví hora and Magdaléna). Technical Report 65, Správa úložišť radioakt. odpadů, Praha, 2016.

[10] BUKOVSKÁ, Z., I. SOEJONO, L. VONDROVIC, M. VAVRO, K. SOUČEK, D. BURIÁNEK, O. ŠVAGERA, P. WACLAWIK, J. ŘIHOŠEK, K. VERNER, J. SLÁMA, L. VAVRO, P. KONÍČEK, L. STAŠ, Z. PÉCSKAY and F. VESELOVSKÝ. Characterization and 3D visualization of underground research facility for deep geological repository experiments: A case study of underground research facility Bukov, Czech Republic. *Engineering Geology*. 2019, 259, 105186. DOI: 10.1016/j.enggeo.2019.105186.

[11] HAKALA, M., H. KUULA and J.A. HUDSON. Estimating the transversely isotropic elastic intact rock properties for in situ stress measurement data reduction: A case study of the Olkiluoto mica gneiss, Finland. *International Journal of Rock Mechanics and Mining Sciences*. 2007. 44, 1, pp.14-46. DOI: 10.1016/j.ijrmms.2006.04.003.

[12] AMADEI, B. Importance of anisotropy when estimating and measuring in situ stress in rock. *International Journal of Rock Mechanics and Mining Sciences & Geomechanics Abstracts*. 1996, 33, 3, pp.293-325. DOI: 10.1016/0148-9062(95)00062-3.

[13] WOROTNICKI, G. CSIRO Triaxial Stress Measurement Cell. *Rock Testing and Site Characterization (Ed.: HUDSON, J.A.)*, 1993. pp.329-394. DOI: 10.1016/B978-0-08-042066-0.50020-3.

[14] KRMÍČEK, L., J. CEMPÍREK, A. HAVLÍN, A. PŘICHYSTAL, S. HOUZAR, M. KRMÍČKOVÁ and P. GADAS. Mineralogy and petrogenesis of a Ba–Ti–Zr-rich peralkaline dyke from Šebkovice (Czech Republic): recognition of the most lamproitic Variscan intrusion. *Lithos*, 2011. 121, pp.74-86. DOI: 10.1016/j.lithos.2010.10.005.

[15] ZANG, A. and O. STEPHANSSON *Stress Fields of the Earth's Crust.* Berlin: Springer, 2010. DOI: 10.1007/978-1-4020-8444-7.

[16] WALTON, G., M. LATO, H. ANSCHÜTZ, M.A. PERRAS and M.S. DIEDERICHS. Non-invasive detection of fractures, fracture zones, and rock damage in a hard rock excavation - Experience from the Äspö Hard Rock Laboratory in Sweden. *Engineering Geology.* 2015, 196, pp. 210-221. DOI: 10.1016/j.enggeo.2015.07.010.

[17] ŠUJANSKÁ, D., M. ZÁVACKÝ and L. KRMÍČEK. Behaviour of syenite under triaxial load conditions. 18th *International Multidisciplinary Scientific GeoConference SGEM.* 2018. Sofie, Bulgaria: STEF92 Technology. 2018. ISSN: 1314–2704, ISBN: 978-619-7408-36-2. DOI: 10.5593/sgem2018/1.2/S02.018.

[18] FIALA, J., G. FUCHS and J.I. WENDT. Moldanubian Zone–stratigraphy. In: DALLMEYER, R.D., W. FRANKE and K. WEBER (Eds.): *Pre-Permian Geology of Central and Eastern Europe*. Berlin: Springer-Verlag, 1995. pp. 417-428. DOI: 10.1007/978-3-642-77518-5.

[19] CEMPÍREK, J., M. NOVÁK, Z. DOLNÍČEK, J. KOTKOVÁ and R. ŠKODA. Crystal chemistry and origin of grandidierite, ominelite, boralsilite, and werdingite from the Bory Granulite Massif, Czech Republic. *American Mineralogist*. 2010, 95, 10, pp.1533-1547. DOI: 10.2138/am.2010.3480.

[20] MERLET, C. Quantitative electron probe microanalysis: new accurate Φ (ρz) description. *Microchimica Acta*. 1992. 12, pp.107-115. DOI: 10.1007/978-3-7091-6679-6_8.

[21] WHITNEY, D.L. and B.W. EVANS. Abbreviations for names of rock-forming minerals. *American mineralogist*. 2010. 95, 1, pp.185-187. DOI: 10.2138/am.2010.3371.

[22] AYDIN, A. Upgraded ISRM Suggested Method for Determining Sound Velocity by Ultrasonic Pulse Transmission Technique. In: ULISAY, R. (Eds.): *The ISRM Suggested Methods for Rock Characterization, Testing and Monitoring: 2007–2014*. Wien: Springer-Verlag. 2014, pp.95-99. DOI: 10.1007/978-3-319-07713-0.

[23] FRANKLIN, J.A. Suggested Methods for Determining the Strength of Rock Materials in Triaxial Compression: Revised Version. *International Journal of Rock Mechanics and Mining Sciences & Geomechanics Abstracts*. 1983, 20, 6, pp.285-290.

[24] BLÜMEL, M. Improved Procedures for Laboratory Rock Testing. In: DGGT (Eds.): *Proceedings of the EUROCK 2000 Symposium*, Aachen. 27-31. Glückauf, Essen, 2000. pp. 573-578.

[25] HOEK, E. and E.T. BROWN. The Hoek-Brown failure criterion and GSI – 2018 edition. *Journal of Rock Mechanics and Geotechnical Engineering*. 2019. 11, 3, pp. 445-463. DOI: 10.1016/j.jrmge.2018.08.001.

[26] OUCHTERLONY, F. Suggested methods for determining the fracture toughness of rock. *International Journal of Rock Mechanics and Mining Sciences and Geomechanics Abstracts*. 1988. 25, 2, pp. 71-96.

[27] RIEDER, M. et al. Nomenclature of the micas. *Clays and Clay Minerals.* 1998, 46, pp.586-595. DOI: 10.1346/CCMN.1998.0460513.

[28] BROSCH, F.J., K. SCHACHNER, M. BLÜMEL, A. FASCHING and H. FRITZ. Preliminary investigation results on fabrics and related physical properties of an anisotropic gneiss. *Journal of Structural Geology*. 2000, 22, pp.1773-1787. DOI: 10.1016/S0191-8141(00)00106-1.

[29] ISRM. Suggested Methods for the Quantitative Description of Discontinuities in Rock Masses. *International Journal of Rock Mechanics and Mining Sciences & Geomechanics Abstracts*. 1978, 15, 6, pp. 319-368.

[30] BROWN, G.J. and D.J. REDDISH. Experimental relations between rock fracture toughness and density. *International Journal of Rock Mechanics and Mining Sciences*. 1997. 34, 1, pp.153-155. DOI: 10.1016/S1365-1609(97)80042-1.

[31] PETRUŽÁLEK, M. *Determination of mechanical properties of the main petrographic types on potential locations of deep repository*. Technical report 88/2017, Geological Institute of the Czech Academy of Science, Prague, 2017.

Volume LXV (2019), No. 4
p. 38 – 53, ISSN 1802-5420
DOI 10.35180/gse-2019-0022